Unsteady State Modeling of an Organic Rankine Cycle for Waste Heat Recovery from Internal Combustion Engine

MAHDI HATF KADHUM ABOALTABOOQ[12]*, TUDOR PRISECARU[1], HORATIU POP[1], VALENTIN APOSTOL[1], VIOREL BADESCU[1], MALINA PRISECARU[1], ELENA POP[1], MIHAELA - CRISTINA CIOBANU[1], MADALINA GHILVACS[1], GHEORGHE POPESCU[1], CRISTIAN PETCU[3], ANA-MARIA ALEXANDRU[1]

[1] University of Politehnica Bucharest, 313 Splaiul Independentei, 060042, Bucharest, Romania

[2] AL-Furat Al-Awsat Technical University, Technical College Najaf, Iraq

[3] Rokura Company, 46-48 Rahmaninov Str., Bucharest, Romania

This paper describes the behavior of an ORC used to recover energy from a variable flow rate and temperature waste heat source from a diesel engine. A steady state model is unable to predict transient behavior in a cycle with a varying thermal source. A Transient model of the ORC is therefore proposed focusing specifically on the time-varying performance of the heat exchangers, the dynamics of the other components being of minor importance. A mathematical model was developed with regard to the preheater, boiler and the superheater zones of a counter flow evaporator. Each of these zones has been subdivided into a number of the cells. ORC unit under investigation uses R245fa as the working fluid. The results show that when heat source decreases the area of zones in heat exchanger are shifted from place to another place. In our case the area of superheater and preheater zones in evaporator is decrease with time, but the boiler zone is increased. In addition, the area of desuperheater in condenser is decrease with time, but the condenser zone is increased. In another words, when the heat source decreases in the evaporator with time, and the mass flow rate of refrigerant is constant that is lead to disappear the superheater zone in evaporator and shift to the boiler zone.

Keywords: waste heat recovery, organic Rankine cycle, transient condition model

The interest in low temperature in the waste heat recovery has grown significantly in the recent decades.

Organic Rankine cycle (ORC) system is one of most promising solutions used to generate electricity from low temperature heat sources. ORC system operates as a classic Rankine cycle but instead of water the organic fluids are used such as R245fa, R123, R113, etc. Yiping Dai et al. [1] studied the effects of the thermodynamic parameters on the ORC performance. The optimum performance of cycles with different working fluids was compared and analyzed under the same waste heat condition. Maogang He et al. [2] presented a steady-state experiment, energy balance and exergy analysis of exhaust gas in order to improve the recovery of the waste heat of an internal combustion engine (ICE). Considering the different characteristics of the waste heat of exhaust gas, cooling water, and lubricant, a combined thermodynamic cycle for waste heat recovery of ICE is proposed. Guopeng Yu et al. [3] presented a simulation model based on an actual Organic Rankine Cycle (ORC) bottoming system of a diesel engine. Simulations and thermodynamic analyses are conducted to observe the influence of evaporating pressure and diesel engine (DE) conditions on system performance. Results indicate that, approximately 75% and 9.5% of waste heat from exhaust gas and from jacket water respectively can be recovered under the engine conditions ranging from high load to low load. Combined with bottoming ORC system, thermal efficiency of diesel engine can be improved up to 6.1%.

Waste heat recovery (WHR) combined with ORC have been studied in a number of previous works: Gu et al. [4], Dai et al. [5], and Badr et al. [6], used simple thermodynamic models with constant pump and expander efficiencies to compare different candidate working fluids. They showed that the cycle efficiency is very sensitive to the evaporating pressure, and that the optimal working fluid depends strongly on the considered application. Advanced cycle configurations have also been studied: Gnutek et al. [7] proposed an ORC cycle with multiple pressure levels and sliding vane expansion machines using R123 in order to maximize the use of the heat source; Chen et al. [8] studied the trans critical CO2 power cycle as an alternative to the ORC cycle using R123 and showed that the generated output power is slightly higher with the trans critical cycle.

It is observed from the literature review that an insignificant amount of research has been done on the unsteady state condition in Organic Rankine cycle systems (ORC) compared to steady state condition. Many steady state models of ORC system have been proposed in literature [9-18]. They have the advantage of simplicity, thus requiring low computing time. Therefore, the focus of this paper will be on unsteady state condition to recover the acute shortage in the literatures in addition to the study will be to know the reaction of ORC in transient condition. Transient analysis is performed using the transient heat exchanger models for both components evaporator and condenser but steady state models for both pump and expander components. This is true because the fact that the response time of the turbo machines are supposed to be very small compared with the heat exchanger.

The present work focuses on ORC operating with variable heat sources. This heat source is considered any heat source, but in our case the waste heat from internal combustion engine (ICE) was used. The specification of ICE is shown in table 1.

The objective of this paper is to create and develop the mathematical model for ORC combining with ICE in

* *email: hatfmahdi@yahoo.com*

Parameter	Specification	Units
Engine type (model)	4-Cylinder	
Power	37.7	kW
Piston stroke, S	110	mm
Compression ratio	18:1	-
Fuel LHV	43	MJ/kg
Exhaust gas temperature	327-477	°C
Cylinder diameter, D	98	mm
Rotation speed	1500	rot/min
Flue gas mass flow rate	160-192.2	kg/h
Water jacket flow rate	327.6-1105.5	kg/h

Table 1
MAIN ENGINE CHARACTERISTICS [19]

unsteady state condition to show the effect of variable heat source with time depending on the optimum evaporation pressure that leads to optimum power of the ORC system. There are two scenarios to overcome the problem:

- constant Refrigerant mass flow rate value with time.;
- variable Refrigerant mass flow rate value for return to the original condition (optimum condition) to produce optimum output power from ORC system.

The mathematical model is simulated by a code developed using MATLAB (R2012a version). The strategy aims to adjust the effect of mass flow rate of refrigerant in order to achieve optimum output power from expander. The mass flow rate of refrigerant and mass flow rate of cooling water in condenser are used as control parameters in this strategy.

Unsteady state modeling

Transient models of both heat exchangers are required for evaporator and condenser when the heat source varies with time. On the other hand, both the pump (process 1–2) and the expander (process 3–4) are considered with static models because of faster response of devices (pump and expander) than heat transfer devices (evaporator and condenser). A finite volume discretization approach for the heat exchanger was used to simulate the behavior of the evaporator as shown in figure 1.

General Overview

The evaporator, which length is L, was divided into N volumes (axial discretization) with length Δx. Each element defines a control volume according to the finite volume method of discretization. For each discrete volume three nodes can be defined in the radial direction: one referring to the fluid within the internal pipe in our case working fluid (referred to as ref) one to the state of the metal constituting the metal wall pipe (referred to as w) one referring to the state of the fluid in the annulus in our case exhaust gases (gas), according to figure 1. The discretization adopted therefore brings to a 2D model since variation of state parameters are evaluated both in the axial and radial direction. The discretization nodes are located at the center of the different control cells that have been identified for the pipe and the two fluids.

For each volume and at each instant of simulation time t energy conservation equations was applied to both the metal pipe and the two fluids.

The assumptions introduced in the analysis of the evaporator are the following:

- thermodynamic properties of both the metal pipe and the working fluid are function of space and time;
- thermal capacitance of both the metal pipe and the fluid are considered;
- the external pipe is assumed to be ideally insulated hence heat losses are neglected;
- head losses are neglected for both the pipes;

The unsteady state modeling was divided in to two parts as follows:

Evaporator model

The area of evaporator will divided in to three zones depending on the design areas [20] and each zone will be divided into many areas. Evaporator was divided into three main zones preheater, boiler and superheater and the area of each zone was calculated. This division is not enough for determining the heat transfer coefficient and the properties of the evaporator and so on. Therefore, each zone in evaporator was divided into a number of cells as follows:

- preheater zone was divided into 60 nodes or (N_{pr}-1) cells;

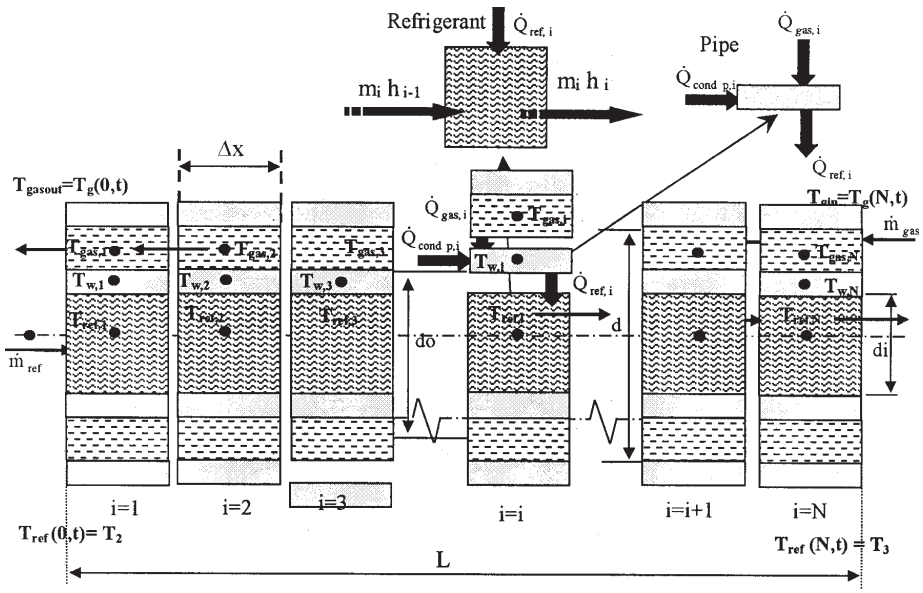

Fig.1. Finite volume representation of the heat exchanger

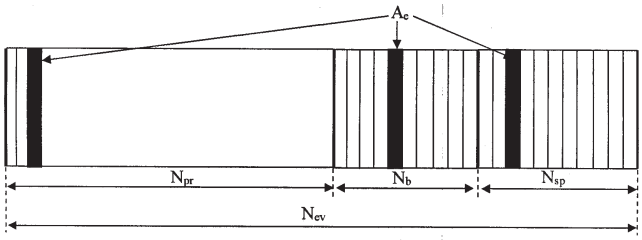

Fig. 2. Evaporator division representation

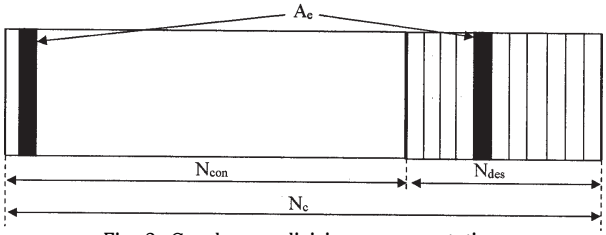

Fig. 3. Condenser division representation.

Parameter	Symbol	Value	Unit
Evaporator area	A_{ev}	2.215	m^2
Preheater area	A_{pr}	1.6756	m^2
Boiler area	A_b	0.2556	m^2
Superheater area	A_{sp}	0.284	m^2
Total length of evaporator	L_{etot}	17.62	m
Preheater length	L_{pr}	13.33	m
Boiler length	L_b	2.034	m
Superheater length	L_{sp}	2.26	m
Outside diameter of the outer tube	d	0.6	m
Outside diameter of the inner tube	d_o	0.4	m
Inside diameter of the inner tube	d_i	0.3	m

Table 2
EVAPORATOR MODEL PARAMETERS FROM DESIGN [21]

Parameter	Symbol	Value	Unit
Total condenser area	A_c	2.384	m^2
Desuperheater area	A_{des}	0.284	m^2
Condenser area	A_{con}	2.1	m^2
Total length of condenser	L_{ctot}	18.97	M
Desuperheater length	L_{des}	2.26	M
condenser length	L_{con}	16.71	M
Outside diameter of the outer tube	d	0.6	M
Outside diameter of the inner tube	d_o	0.4	M
Inside diameter of the inner tube	d_i	0.3	M

Table 3
CONDENSER MODEL PARAMETERS FROM DESIGN [21]

- Boiler zone was divided into 10 nodes or (N_b-1) cells;
- superheater zone was divided into 11 nodes or (N_{sp}-1) cells as shown in figure 2.

The energy equation is applied (fig. 1).

For each cell, a heat exchange area and a fluid volume are defined:

$$A_e = \frac{A_{pr}}{N_{pr}-1} = \frac{A_{br}}{N_b-1} = \frac{A_{sp}}{N_{sp}-1} \qquad V_e = \frac{V_{pr}}{N_{pr}-1} = \frac{V_{br}}{N_b-1} = \frac{V_{sp}}{N_{sp}-1}$$

$$N_{bp} = N_{pr+} N_b$$

$$N_{ev} = N_{pr} + N_b + N_{sp} = N_{bp} + N_{sp}$$

where:

A_e is the element area, V_e is the element volume, N_{bp} is the number of nodes in preheater and boiler zone, N_{ev} is the number of nodes in all zones of evaporator.

The area of evaporator is equal to summation of preheater, boiler and superheater zones. On the other hand, the area of the condenser is equal to summation of desuperheater and condenser zones.

Condenser model

Condenser was divided into two main zones desuperheater and condenser and the area of each zone was calculated. This division is not enough for determining the heat transfer coefficient and the properties of the condenser. Therefore, each zone in condenser was divided into a number of cells as follows:

- desuperheater zone was divided into 11 nodes or (N_{des}-1) cells;
- condenser zone was divided into 75 nodes or (N_{con}-1) cells as shown in figure 3.

$$N_c = N_{des} + N_{con}$$

where N_{des} is the number of nodes in desuperheater zone, N_{con} is the number of nodes in condenser zone; N_c is the number of nodes in all zones of condenser.

Energy balance for exhaust gases (heat source)

General energy balance equation for exhaust gas side is represented by equation (1)

$$\frac{\partial E_{g,i}}{\partial t} = \dot{Q}_{g,i}^{t+\Delta t} - \dot{Q}_{g,i}^{t} \quad (1)$$

where:

$$\frac{\partial E_{g,i}}{\partial t} = \frac{\Delta E_{g,i}}{\Delta t} = \frac{E_{g,i}^{t+\Delta t} - E_{g,i}^{t}}{(t+\Delta t)-(t)} \quad (2)$$

$$E_{g,i}^{t+\Delta t} = V_g \rho_g Cp_g T_{g,i}^{t+\Delta t} \quad (3)$$

$$E_{g,i}^{t} = V_g \rho_g Cp_g T_{g,i}^{t} \quad (4)$$

V_g is the volume of the exhaust gas for the cell, ρ_g is the density of the exhaust gas for the cell, Cp_g is the specific heat of the exhaust gas for the cell, $\dot{Q}_{g,i}^{t+\Delta t}$ is the energy of exhaust gas at ($t+\Delta t$). $\dot{Q}_{g,i}^{t}$ is the energy of exhaust gas at (t). $T_{g,i}^{t}$ is the temperature of the exhaust gas for the cell at time (t), $T_{g,i}^{t+\Delta t}$ is the temperature of the exhaust gas for the cell at new time ($t+\Delta t$), Δt is the time step.

Substitute equation (3) and (4) in equation (2) we will get equation (5):

$$\frac{\Delta E_{g,i}}{\Delta t} = \frac{V_g \rho_g Cp_g T_{g,i}^{t+\Delta t} - V_g \rho_g Cp_g T_{g,i}^{t}}{(t+\Delta t)-(t)} = \frac{V_g \rho_g Cp_g \left(T_{g,i}^{t+\Delta t} - T_{g,i}^{t}\right)}{\Delta t} \quad (5)$$

Energy balance equation for the exhaust gases in time (t):

$$\dot{Q}_{g,i}^{t} = \dot{m}_g Cp_g \left(T_{g,i-1}^{t} - T_{g,i}^{t}\right) = H_g A_e \left(T_{g,i}^{t} - T_{w,i}^{t}\right)_{cell} \quad (6)$$

Energy balance equation for the exhaust gases in time (t+Δt):

$$\dot{Q}_{g,i}^{t+\Delta t} = \dot{m}_g\, Cp_g \left(T_{g,i-1}^{t+\Delta t} - T_{g,i}^{t+\Delta t}\right) = H_g\, A_e \left(T_{g,i}^{t+\Delta t} - T_{w,i}^{t+\Delta t}\right)_{cell} \quad (7)$$

Substitute equation (5), (6) and (7) in equation (1) we will get equation (8):

$$\frac{V_g\, \rho_g\, Cp_g \left(T_{g,i}^{t+\Delta t} - T_{g,i}^{t}\right)}{\Delta t} = H_g\, A_e \left(T_{g,i}^{t+\Delta t} - T_{w,i}^{t+\Delta t}\right)_{cell} - H_g\, A_e \left(T_{g,i}^{t} - T_{w,i}^{t}\right)_{cell} \quad (8)$$

We can determine from equation (8) the wall temperature in new time depending on exhaust gases temperature in old and new time.

Energy balance for wall

General energy balance equation for wall side is represented by equation (9)

$$\frac{\partial E_{w,i}}{\partial t} = \dot{Q}_{g\text{-}w,i}^{t+\Delta t} - \dot{Q}_{w\text{-}ref,i}^{t} \quad (9)$$

$$\frac{\partial E_{w,i}}{\partial t} = \frac{\Delta E_{w,i}}{\Delta t} = \frac{E_{w,i}^{t+\Delta t} - E_{w,i}^{t}}{(t+\Delta t) - (t)} \quad (10)$$

$$E_{w,i}^{t+\Delta t} = m_{w,i}\, C_w\, T_{w,i}^{t+\Delta t} \quad (11)$$

$$E_{w,i}^{t} = m_{w,i}\, C_w\, T_{w,i}^{t} \quad (12)$$

$m_{w,i}$ is the mass of the wall for the cell, C_w is the specific heat of the wall for the cell, $T_{w,i}^{t}$ is the temperature of the wall for the cell at time (t), $T_{w,i}^{t+\Delta t}$ is the temperature of the wall for the cell at time (t+Δt). $\dot{Q}_{g\text{-}w}^{t+\Delta t}$ is the energy leave from exhaust gas to the wall at time (t+Δt) $\dot{Q}_{w\text{-}ref,i}^{t}$ is the energy leave from the wall to the refrigerant at time (t).

Substitute equation (11) and (12) in equation (10), we will get equation (13):

$$\frac{\Delta E_{w,i}}{\Delta t} = \frac{m_w\, C_w\, T_{w,i}^{t+\Delta t} - m_w C_w\, T_{w,i}^{t}}{(t+\Delta t) - (t)} = \frac{m_w\, C_w \left(T_{w,i}^{t+\Delta t} - T_{w,i}^{t}\right)}{\Delta t} \quad (13)$$

Energy balance equation for the wall in time (t):

$$\dot{Q}_{g\text{-}w,i}^{t} = \dot{m}_g\, Cp_g \left(T_{g,i-1}^{t} - T_{g,i}^{t}\right) = \dot{m}_{ref} \left(h_{ref,i+1}^{t} - h_{ref,i}^{t}\right) \quad (14)$$

Or:

$$\dot{Q}_{g\text{-}w,i}^{t} = H_g\, A_e \left(T_{g,i}^{t} - T_{w,i}^{t}\right)_{cell} = H_{ref}\, A_e \left(T_{w,i}^{t} - T_{ref,i}^{t}\right)_{cell} \quad (15)$$

Energy balance equation for the wall in time (t+Δt):

$$\dot{Q}_{w\text{-}ref,i}^{t+\Delta t} = \dot{m}_g\, Cp_g \left(T_{g,i-1}^{t+\Delta t} - T_{g,i}^{t+\Delta t}\right) = \dot{m}_{ref} \left(h_{ref,i+1}^{t+\Delta t} - h_{ref,i}^{t+\Delta t}\right) \quad (16)$$

Or:

$$\dot{Q}_{w\text{-}ref,i}^{t+\Delta t} = H_g\, A_e \left(T_{g,i}^{t+\Delta t} - T_{w,i}^{t+\Delta t}\right)_{cell} = H_{ref}\, A_e \left(T_{w,i}^{t+\Delta t} - T_{ref,i}^{t+\Delta t}\right)_{cell} \quad (17)$$

Substitute equation (13), (15) and (17) in equation (9), we will get equation (18):

$$\frac{m_w\, C_w \left(T_{w,i}^{t+\Delta t} - T_{w,i}^{t}\right)}{\Delta t} = H_{ref}\, A_e \left(T_{w,i}^{t+\Delta t} - T_{ref,i}^{t+\Delta t}\right)_{cell} - H_{ref}\, A_e \left(T_{w,i}^{t} - T_{ref,i}^{t}\right)_{cell} \quad (18)$$

We can determine from equation (18) the refrigerant temperature in new time depending on wall temperature in old and new time.

Energy balance for refrigerant

General energy balance equation for refrigerant side is represented by equation (19)

$$\frac{\partial E_{ref,i}}{\partial t} = \dot{Q}_{ref,i}^{t+\Delta t} - \dot{Q}_{ref,i}^{t} \quad (19)$$

$$\frac{\partial E_{ref,i}}{\partial t} = \frac{\Delta E_{ref,i}}{\Delta t} = \frac{E_{ref,i}^{t+\Delta t} - E_{ref,i}^{t}}{(t+\Delta t) - (t)} \quad (20)$$

$$E_{ref,i}^{t+\Delta t} = V_{ref}\, \rho_{ref}\, h_{ref,i}^{t+\Delta t} \quad (21)$$

$$E_{ref,i}^{t} = V_{ref}\, \rho_{ref}\, h_{ref,i}^{t} \quad (22)$$

V_{ref} is the volume of the refrigerant for the cell, ρ_{ref} is the density of the refrigerant for the cell, $h_{ref,i}^{t+\Delta t}$ is the enthalpy of the refrigerant for the cell at time (t+Δt), $h_{ref,i}^{t}$ is the enthalpy of the refrigerant for the cell at time (t). $\dot{Q}_{ref,i}^{t+\Delta t}$ is the energy of the refrigerant at time (t+Δt). $\dot{Q}_{ref,i}^{t}$ is the energy of the refrigerant at time (t).

Substitute equation (21) and (22) in equation (20), we will get equation (23):

$$\frac{\Delta E_{ref,i}}{\Delta t} = \frac{V_{ref}\, \rho_{ref}\, h_{ref,i}^{t+\Delta t} - V_{ref}\, \rho_{ref}\, h_{ref,i}^{t}}{\Delta t} = \frac{V_{ref}\, \rho_{ref} \left(h_{ref,i}^{t+\Delta t} - h_{ref,i}^{t}\right)}{\Delta t} \quad (23)$$

Energy balance equation for the working fluid in time (t):

$$\dot{Q}_{ref,i}^{t} = \dot{m}_{ref} \left(h_{ref,i+1}^{t} - h_{ref,i}^{t}\right) = H_{ref}\, A_e \left(T_{w,i}^{t} - T_{ref,i}^{t}\right)_{cell} \quad (24)$$

Energy balance equation for the working fluid in time (t+Δt):

$$\dot{Q}_{ref,i}^{t+\Delta t} = \dot{m}_{ref} \left(h_{ref,i+1}^{t+\Delta t} - h_{ref,i}^{t+\Delta t}\right) = H_{ref}\, A_e \left(T_{w,i}^{t+\Delta t} - T_{ref,i}^{t+\Delta t}\right)_{cell} \quad (25)$$

Substitute equation (23), (24) and (25) in equation (19), we will get equation (26):

$$\frac{V_{ref}\, \rho_{ref} \left(h_{ref,i}^{t+\Delta t} - h_{ref,i}^{t}\right)}{\Delta t} = H_{ref}\, A_e \left(T_{w,i}^{t+\Delta t} - T_{ref,i}^{t+\Delta t}\right)_{cell} - \dot{m}_{ref} \left(h_{ref,i+1}^{t} - h_{ref,i}^{t}\right) \quad (26)$$

We can determine from equation (26) the refrigerant enthalpy in time (t+Δt) depending on wall temperature and refrigerant temperature in time (t+Δt).

Working fluid model

Curve fitting in Matlab

In order to be able to investigate an Organic Rankine Cycle (ORC), the state properties of the working fluid, which is R245fa in our situation, are required to be evaluated. A sample property can be computed using following equation:

$$y = a_n\, P^n + a_{n-1}\, P^{n-1} + a_{n-2}\, P^{n-2} + a_{n-3}\, P^{n-3} + \ldots\ldots + a_0\, P^0 \quad (27)$$

where y represents the thermo-physical property, a_n to a_0 are the regressed constants.

Error in curve fitting

The errors of curve fitting were calculated as shown in table 5.

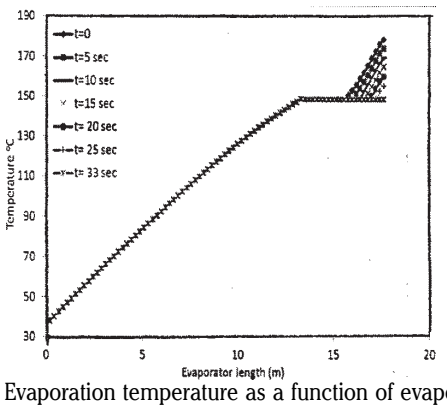

Fig. 4. Evaporation temperature as a function of evaporation pressure

Property	Dependent variable	a_7	a_6	a_5	a_4	a_3	a_2	a_1	a_0
Evap.temp.(T_{ev})	P_{ev}	——	$-1*10^{-6}$	0.00013	-0.0067	0.17	-2.5	22	-5
Pressure (P_1)	T_1	——	$-1.2*10^{-}$	$2*10^{-8}$	$-1.2*10^{-6}$	$3.7*10^{-5}$	0.00016	0.021	0.59
Entropy (S_1)	T_1	——	——	——	——	——	$-2*10^{-6}$	0.0046	1
Enthalpy (h_1)	T_1	——	——	——	$-7.3*10^{-7}$	$9*10^{-5}$	-0.0019	1.3	200
Enthalpy (h_2)	S_1	——	——	——	——	37	-14	1900	-10
Temperature	h_2	——	——	——	——	$2.2*10^{-6}$	-0.0023	1.5	-220
Entropy (S_3)	P_{ev}	——	——	——	——	$2.3*10^{-6}$	-0.0002	0.0078	1.8
Enthalpy (h_3)	P_{ev}	$-8.8*10^{-7}$	0.00011	-0.0057	0.0057	0.15	-2.2	20	4300
Enthalpy (h_{2sat})	T_{ev}	$1.4*10^{-11}$	$-8.6*10^{-9}$	$2.1*10^{-6}$	-0.00028	0.02	0.82	18	84
Enthalpy (h_{3sat})	T_{ev}	$1.4*10^{-11}$	$8.4*10^{-9}$	$-2.1*10^{-6}$	0.00027	-0.02	0.79	-15	5200
Temperature	S_3	——	——	——	——	——	26	2400	-4700
Enthalpy (h_5)	T_1	——	——	——	——	$-2.5*10^{-5}$	0.0025	0.7	4100

Table 4
COEFFICIENTS OF PROPERTY EQUATION FOR R245fa

Property	*Actual By EES*	*Obtained By curve fitting*	*Relative error [%]*
Evaporation temperature (°C)	147.985	148.181	+ 0.1322
Enthalpy at inlet turbine (kJ/kg)	556.649	556.722	+0.0131
Enthalpy at point (2 sat) (kJ/kg)	435.139	435.878	+0.169
Enthalpy at point (3 sat) (kJ/kg)	494.789	491.615	-0.641
Entropy at inlet turbine (kJ/kg.K)	1.951	1.9505	-0.0256
Temperature of point (4) (°C)	98.625	98.466	-0.161
Enthalpy at point (4) (kJ/kg)	496.417	496.313	-0.0209

Table 5
RELATIVE ERRORS IN R245fa PROPERTY CALCULATIONS

For establishing the equation of state, data of thermodynamic properties of the selected fluid (R245fa) as example evaporation temperature, enthalpy, entropy, density and pressure for the ORC system was plotted in MATLAB 12, and curve fitting was performed with the minimum residual as shown in the figure (4) as example.

Result and discussions

The simulation model described in section 2 was tested with different heat source. A simulation is run for two scenarios and for working fluid (R245fa) at constant evaporating pressure and temperature respectively (32.57 bar, 148°C) in order to compare their respective performance.

First scenario (constant refrigerant mass flow rate)

When the system is operate in the first scenario, and the heat source temperature decreases gradually the results show that superheater zone area starts to decrease until all superheater zone disappear and the total area of superheater added to boiler zone area as well as that preheater zone was decreased and the difference between the new area of preheater and old area shall be added to boiler zone also.

Figure 5 shows that refrigerant temperature of superheater zone (in point 3) decreases with time step by

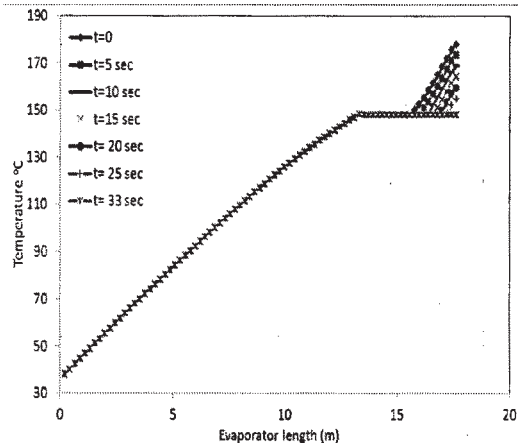

Fig. 5. Refrigerant temperature variation with evaporator tube under unsteady state condition

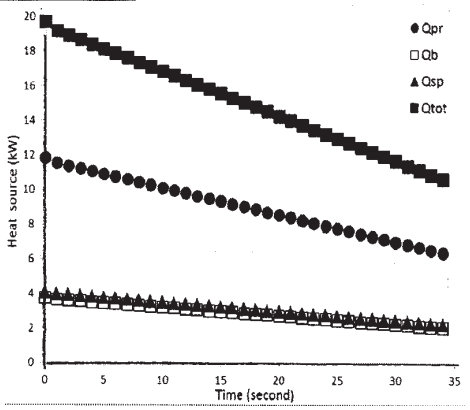

Fig. 6. Heat source energy variation with time.

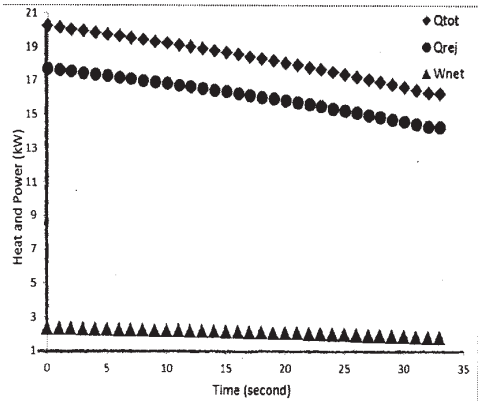

Fig. 7 Heat source, work net and heat rejected variation with time

step until the temperature of superheater zone is equal to evaporation temperature after 33 s due to decreasing of heat source, and the mass flow rate of refrigerant is constant. Therefore, in this condition the mass flow rate of refrigerant must be changed to new value in order to avoid the situation of no superheating in our system.

The heat source variation with time is shown in figure (6) as a sample from 100 % load decreases toward 75 % load. The heat source for each zone and the total heat source are explained. Figure 7 shows that the heat source energy, work net and heat rejected variations with time. Clearly that the work net and heat rejected is decrease with time due to heat source decrease. The area of

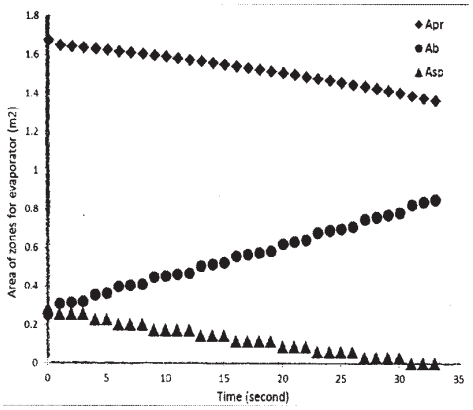

Fig. 8. Area of evaporator zones for variation with time.

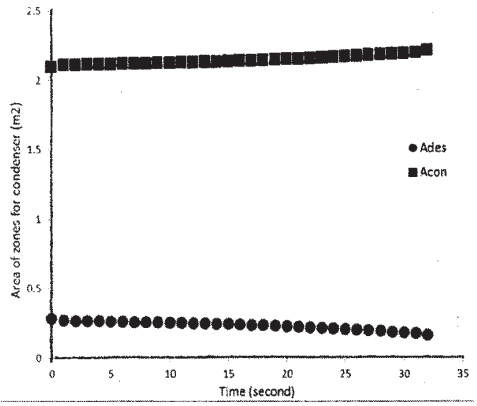

Fig. 9. Area of condenser zones for variation with time

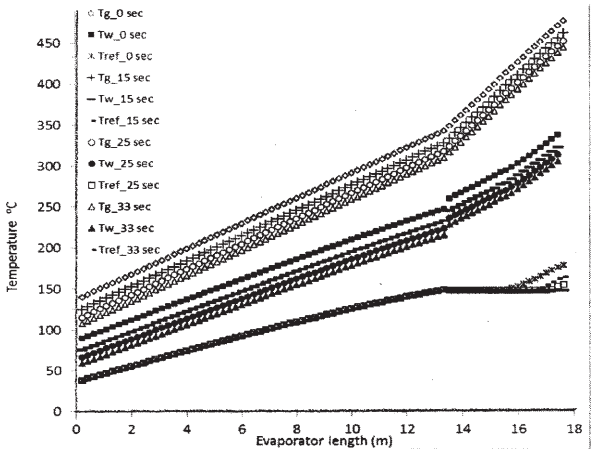

Fig. 10. The temperature of heat source, wall and refrigerant along evaporator tube under time variations

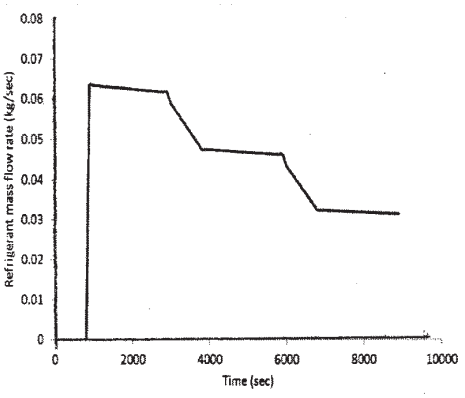

Fig. 11. Refrigeration mass flow rate variations with time

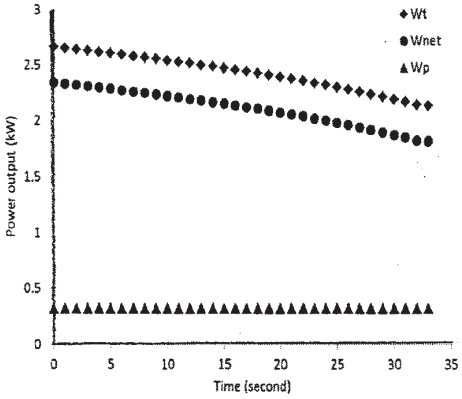

Fig. 12. Variation of turbine work, work net and pump work of ORC with time.

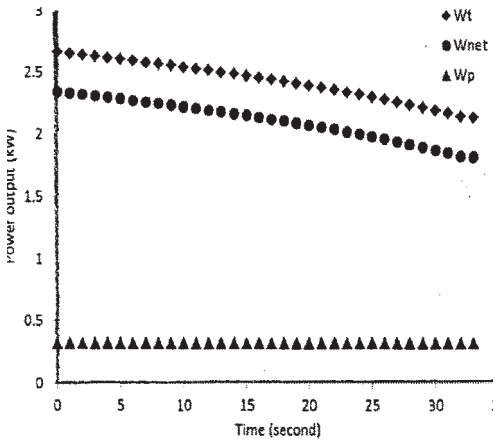

Fig. 13. Effect of increasing mass flow rate on Evaporator fluid zones

preheater, boiler and superheater zone variations with time is shown in figure 8. It is clear from that figure the area of superheater zone is decreases with time until all area is shift into boiler zone. The area of preheater zone is decreases with time and vice versa for boiler zone. Figure 9 shows that area of zones for condenser variation with time.

Figure 10 shows the temperature of heat source, wall and refrigerant a long evaporator tube under time variations. It is clear from figure the temperature of the wall takes the same mode of heat source but the temperate of refrigerant is decreases with heat source, and wall temperature is decreases until reach the evaporation temperature if the mass flow rate of refrigerant is constant. Therefore, this situation needs to process in order to maintain a system works with more efficient.

Second scenario (variable refrigerant mass flow rate)

First scenario shows that the system was operated under limited time because the dropping in heat source and mass flow rate of refrigerant is constant. After that the system must be shut down or handling the system to work in all time. The only one solution for this problem change the mass flow rate of refrigerant by change the speed of the pump to maintain the refrigerant in superheating form to avoid dangerous for wet refrigerant inside the turbine. In our case, the mass flow rate must be decreased to give chance for refrigerant to transfer into superheater zone as shown in figure 11.

When the heat source is decreases, the point (3) is shift toward the point (3sat), so the work net is decreases. In order to keep the point (3) constant must decrease the mass flow rate of refrigerant. Therefore, the new work net in new time is decreases as shown in figure 12.

As can be seen in figure 13, when the mass flow rate through the evaporator increases and the other parameters

remain constant, the length of the liquid and two-phase zones increase while the superheated zone length decreases. This is because the increase in mass flow rate is not balanced by a proportionate increase in thermal energy added to the working fluid. After increasing the mass flow rate more than normal limit the vapor zone is disappear as shown in figure 13 c.

Conclusions

There are some of the conclusions from this work as follows:

In ORC system when the heat source decreases the area of zones in heat exchanger is shifted from place to another place. As an example, in our case the area of superheater and preheater zones in evaporator is decrease with time, but the boiler zone is increased. In addition, the area of desuperheater in condenser is decrease with time, but the condenser zone is increased.

When the heat source decreases in the evaporator with time, and the mass flow rate of refrigerant is constant that is lead to disappear the superheater zone in evaporator and shift to the boiler zone.

In the same way if the heat rejection in the condenser is decreases with time and the mass flow rate of water to cooling the refrigerant is constant that is lead to decreases the desuperheater zone and shift to the condenser zone.

There is a strategy to control on the ORC system work to be always in the optimum condition through control on the mass flow rate of refrigerant automatically, which means changing the mass flow rate of refrigerant constantly under variation of heat source.

The suddenly decreasing in heat source leads to need less time to reach the dangerous condition.

In this respect, future work will be conducted in order to determine the performance of the ORC under unsteady state condition.

Acknowledgments: The author (M.H.K.Aboaltabooq) acknowledges support from the Iraqi government through grant and the Romanian government through Research grant ," Hybrid micro-cogeneration group of high efficiency equipped with an electronically assisted ORC", 1st Phase Report, 2nd National Plan, Grant Code: PN-II-PT-PCCA-2011-3.2-0059, Grant No.: 75/2012.

References

1. YIPING DAI, JIANGFENG WANG, LIN GAO '' Parametric optimization and comparative study of organic Rankine cycle (ORC) for low grade waste heat recovery '' Energy Conversion and Management, **50**, 2009, P. 576–582.

2. MAOGANG HE, XINXIN ZHANG, KE ZENG, KE GAO ''A combined thermodynamic cycle used for waste heat recovery of internal combustion engine '' Energy, **36**, 2011, P. 6821-6829.

3. GUOPENG YU, GEQUN SHU, HUA TIAN, HAIQIAO WEI, LINA LIU ''Simulation and thermodynamic analysis of a bottoming Organic Rankine Cycle (ORC) of diesel engine (DE)'' Energy, **51**, 2013, P. 281-290.

4. GU W, WENG Y, WANG Y, ZHENGh B. Theoretical and experimental investigation of an organic Rankine cycle for a waste heat recovery system. Proc IMechE, Part A: J Power Energy, **223**, 2009, p.523–533.

5. DAI YP, WANG JF, et al. Parametric optimization and comparative study of organic Rankine cycle (ORC) for low grade waste heat recovery. Energy Convers Manage, **50**, (3), 2009, p. 576–582.

6. Badr O, Ocallaghan PW, et al. Rankine-cycle systems for harnessing power from low-grade energy-sources. Applied Energy 1990; vol. 36 (4):pp. 263–292.

7. GNUTEK Z, BRYSZEWSKA-MAZUREK A. The thermodynamic analysis of multi cycle ORC engine. Energy, **26**, (12), 200, p. 1075–1082.

8. CHEN Y, LUNDQVIST P, et al. A comparative study of the carbon dioxide trans critical power cycle compared with an organic Rankine cycle with R123 as working fluid in waste heat recovery. Applied Thermal Engineering, 26 (17– 18), 2006, p.2142–2147.

9. YU C, CHAU KT. Thermoelectric automotive waste heat energy recovery using maximum power point tracking. Energy Convers Manage, **50**, 2009, pp. 1506-1512.

10. ZHANG A H , et al. Study of working fluid selection of organic Rankine cycle (ORC) for engine waste heat recovery, Energy, **36**, 2011, p.3406-3418.

11. MAGO, P.J., CHAMRA,L.M., SOMAYAJI,C., Performance analysis of different working fluids for use in organic Rankine cycles, Proc. IMechE, **Part** A: J. Power and Energy**, 221**, 2009.

12. ROY,J.P., et al. Performance analysis of an Organic Rankine Cycle with superheating under different heat source temperature conditions, Applied Energy, **88**, 2011, P. 2995–3004.

13. ZHANG,H.G., WANG,E.H., FANB.Y., Heat transfer analysis of a finned-tube evaporator for engine exhaust heat recovery, Energy Conversion and Management, **65**, 2013, P. 438–447.

14. GUOPENG YU, GEQUN SHU, HUA TIAN, HAIQIAO WEI, LINA LIU. Simulation and thermodynamic analysis of a bottoming Organic Rankine Cycle (ORC) of diesel engine (DE). Energy, **51**, 2013, P. 281-290.

15. GHAZI,M, AHMADI,P, SOTOODEH,A.F., TAHERKHANI A. Modeling and thermo economic optimization of heat recovery heat exchangers using a multimodal genetic algorithm. Energy Conversion Manage, **58**, 2012, P. 149–156.

16. PERIS,B., NAVARRO-ESBRI,J., MOLES,F., Bottoming organic Rankine cycle configurations to increase Internal Combustion Engines power output from cooling water waste heat recovery, Applied Thermal Engineering, **61**, 2013, P. 364-371.

17. NAIJUN ZHOU, et al. Experimental study on Organic Rankine Cycle for waste heat recovery from low-temperature flue gas, Energy, **55**, 2013), P. 216-225.

18. DAI Y, et al. Parametric optimization and comparative study of organic Rankine cycle (ORC) for low grade waste heat recovery, Energy Conversion and Management, **50** , 2009, P. 576-582.

19. Research Grant," Hybrid micro-cogeneration group of high efficiency equipped with an electronically assisted ORC", 1st Phase Report, 2nd National Plan, Grant Code: PN-II-PT-PCCA-2011-3.2-0059, Grant No.: 75/2012.

20. MAHDI HATF KADHUM. Optimum Operation Conditions and Behavior of Organic Rankine Cycle System under Variable Heat Input with Control on Refrigerant Mass Flow Rate, third report for PhD study, Politehnica University 2014.

21. MAHDI HATF KADHUM, et al. Parametric investigation study of counter-flow evaporator for waste heat recovery, 3nd International Conference on Thermal Equipment, Renewable Energy and Rural Development, 2014, p. 71-76.

Manuscript received: 15.07.2015